

Steering the energy sharing of electrons in nonsequential double ionization with orthogonally polarized two-color field

Guangqi Fan(樊光琦), Zhijie Yang(杨志杰), Fenghao Sun(孙烽豪), Jinmei Zheng(郑金梅), Yuntian Han(韩云天), Mingqian Huang(黄明谦), and Qingcao Liu(刘情操)

Citation: Chin. Phys. B, 2024, 33 (**8**): 083102. DOI: 10.1088/1674-1056/ad4bc0

What follows is a list of articles you may be interested in

Energy levels and magnetic dipole transition parameters for the nitrogen isoelectronic sequence

Mu-Hong Hu(胡木宏), Nan Wang(王楠), Pin-Jun Ouyang(欧阳品均),Xin-Jie Feng(冯新杰), Yang Yang(杨扬), and Chen-Sheng Wu(武晨晟)
Chin. Phys. B, 2022, 31 (**9**): 093101. DOI: 10.1088/1674-1056/ac7a12

Calculations of atomic polarizability for beryllium using MCDHF method

Hui Dong(董辉), Jun Jiang(蒋军), Zhongwen Wu(武中文), Chenzhong Dong(董晨钟), and Gediminas Gaigalas
Chin. Phys. B, 2021, 30 (**4**): 043103. DOI: 10.1088/1674-1056/abd92d

Accurate all-electron calculation on the vibrational and rotational spectra of ground states for O_2 and its ions

Qiao-Xia Wang(王巧霞), Yu-Min Wang(王玉敏), Ri Ma(马日), Bing Yan(闫冰)
Chin. Phys. B, 2019, 28 (**7**): 073101. DOI: 10.1088/1674-1056/28/7/073101

Interface properties and electronic structures of aromatic molecules with anhydride and thio-functional groups on Ag (111) and Au (111) substrates

Wei-Qi Yu(余维琪), Hong-Jun Xiao(肖红君), Ge-Ming Wang(王戈明)
Chin. Phys. B, 2019, 28 (**10**): 103101. DOI: 10.1088/1674-1056/ab4276

Potential energy curves, transition dipole moments, and radiative lifetimes of KBe molecule

Ming-Jie Wan(万明杰), Cheng-Guo Jin(金成国), You Yu(虞游), Duo-Hui Huang(黄多辉), Ju-Xiang Shao(邵菊香)
Chin. Phys. B, 2017, 26 (**3**): 033101. DOI: 10.1088/1674-1056/26/3/033101

Steering the energy sharing of electrons in nonsequential double ionization with orthogonally polarized two-color field

Guangqi Fan(樊光琦)[1,†], Zhijie Yang(杨志杰)[1,†], Fenghao Sun(孙烽豪)[2,‡], Jinmei Zheng(郑金梅)[3], Yuntian Han(韩云天)[1], Mingqian Huang(黄明谦)[1], and Qingcao Liu(刘情操)[1,§]

[1] *College of Science, Harbin Institute of Technology, Weihai* 264209, *China*
[2] *School of Information Science and Engineering, Harbin Institute of Technology, Weihai* 264209, *China*
[3] *Harbin Institute of Technology, Weihai* 264209, *China*

(Received 11 March 2024; revised manuscript received 3 May 2024; accepted manuscript online 15 May 2024)

Using the semiclassical ensemble model, the dependence of relative amplitude for the recollision dynamics in nonsequential double ionization (NSDI) of neon atom driven by the orthogonally polarized two-color field (OTC) laser field is theoretically studied. And the dynamics in two typical collision pathways, recollision-impact-ionization (RII) and recollision-excitation with subsequent ionization (RESI), is systematically explored. Our results reveal that the V-shaped structure in the correlated momentum distribution is mainly caused by the RII mechanism when the relative amplitude of the OTC laser field is zero, and the first ionized electrons will quickly skim through the nucleus and share few energy with the second electron. As the relative amplitude increases, the V-shaped structure gradually disappears and electrons are concentrated on the diagonal in the electron correlation spectrum, indicating that the energy sharing after electrons collision is symmetric for OTC laser fields with large relative amplitudes. Our studies show that changing the relative amplitude of the OTC laser field can efficiently control the electron–electron collisions and energy exchange efficiency in the NSDI process.

Keywords: nonsequential double ionization, correlated electron–electron momentum distribution, energy sharing of electrons, orthogonally polarized two-color field laser field, semiclassical ensemble models

PACS: 31.15.V–, 32.80.Rm, 34.50.Fa, 34.80.Dp **DOI:** 10.1088/1674-1056/ad4bc0

1. Introduction

During the past decades, photoelectron dynamics has been a topic of wide interest in atomic and molecular physics. As the starting point for ultrafast physics research, the ionization of atoms and molecules driven by strong laser fields has triggered various interesting nonlinear physical phenomena. Such as photoelectron vortex,[1,2] photoelectron holographic interference,[3,4] high-order harmonic generation,[5,6] atomic and molecular orbital imaging,[7,8] Rydberg state excitation[9,10] and nonsequential double ionization (NSDI).[11–13] Among them, NSDI as the fundamental and typical multi-electron ionization phenomenon, gives a broad path to explore and understand the underlying correlations of the photoelectron dynamics. The origin of research on the two-electron ionization can be traced back several decades, and its phenomenon was first observed in 1977. With the first observation of the "knee structure" in experiments[14] and the proposal of the recollision theory model,[15] the highly correlation effect between two electrons in NSDI has drawn wide attention in the past decades. In the recollision model, an electron in an atom first tunnels out and then recollides with the parent ion core after being accelerated by external laser field, finally, resulting in the emission of another electron. Generally, in NSDI, the experimental and theoretical studies have confirmed that two typical collision pathways will coexist in the NSDI process, i.e, recollision-impact-ionization (RII) and recollision-excitation with subsequent ionization (RESI).[16–18] Revealing and manipulating the complicated electron dynamics correlation in NSDI is a central issue in atomic and molecular physics.

Previously, a considerable number of studies have been devoted to revealing the dependence that is intimately connected with both kinematics and the dynamics of the participating electrons in recollision process. Clearly, the direct and powerful way is to manipulate the parameters of the driving field, such as the wavelength and intensity.[19–21] However, a significant portion of studies have been performed on linearly polarized laser field. Recently, the orthogonally polarized two-color field (OTC) has made progress on elliptical high-order harmonic generation.[22,23] The OTC electric field is a tailored laser field that has more adjustable parameters than the linearly polarized laser field. Such as relative amplitude, relative frequency and relative initial phase. As a result, many fascinating spatiotemporal correlation phenomena can be successfully reproduced at the attosecond time scales.[24,25] More intriguingly, experimental and theoretical studies have revealed that a strong dependence between the electron correlation characteristics and the relative initial phase of the OTC electric

[†]These authors contributed equally to this work.
[‡]Corresponding author. E-mail: fhsun@hit.edu.cn
[§]Corresponding author. E-mail: qingcao.liu@hit.edu.cn

© 2024 Chinese Physical Society and IOP Publishing Ltd

field.[26–28]

In this paper, we conduct a theoretical investigation into the double ionization of neon atom in the OTC electric field using the semiclassical ensemble model. Our focus lies on the momentum distribution, which we examine by introducing a relative initial phase of 0.5π and varying the relative amplitude of the OTC electric field to explore the correlation characteristics of recolliding electrons in NSDI. Our results indicate that the asymmetrical energy sharing of electron pairs is reliant on the relative amplitude of the OTC electric field. Notably, an observable trend of symmetrical energy sharing emerges during initial stage of electron collisions as the relative amplitude of the OTC electric field increases. Thus, our studies reveal the energy sharing mechanism that manipulates the electron pairs generated by collisions and systematically analyze this dynamic process using two collision pathways, RII and RESI, respectively.

2. Theoretical simulation details

The ionization of atoms and molecules driven by strong laser fields serves as the foundation of ultrafast physics and facilitates the investigation of quantum microphysics. As the field of ultrafast physics has developed, numerous theoretical models have been proposed consecutively. NSDI, a fundamental and typical phenomenon of multi-electron ionization can be described using several theoretical models. Such as quantum methods that the numerical solution time-dependent schrödinger equation,[29–31] the S-matrix models based on strong field approximation,[32] the classical and semiclassical ensemble models.[33–35]

Due to the trajectory of the electron cannot be tracked through numerical solution time-dependent Schrödinger equation and this approach is highly computationally demanding,[36] numerous studies have resorted to the classical and semiclassical ensemble models in the past decades. The fundamental concept of both models involves representing the actual electron wave function using a vast quantity of model atoms. Established experimental and theoretical studies have demonstrated that both classical and semiclassical models have proven to be highly successful in explaining and predicting a variety of phenomena in NSDI.[33–35]

In contrast to the classical ensemble model, the semiclassical model considers the quantum tunnelling effect of the first electron, and its initial state and ionization probability are described by ADK tunneling theory.[37] The longitudinal velocity of tunneled electron is zero and transverse velocity follows a Gaussian-like distribution with an expected value $\mu = 0$ and a variance $\sigma^2 = E(t_0)/(2\sqrt{2I_{\mathrm{p1}}})$. Here t_0 is the tunneling time, $E(t_0)$ is the transient electric field strength at tunneling and $I_{\mathrm{p1}} = 21.56$ eV is the first ionization potential of neon atom. And the initial state of the bound electron is sampled from the microcanonical distribution base on the second ionization potential $I_{\mathrm{p2}} = 40.96$ eV.[38] The evolution of tunneling electrons in response to combined Coulomb and laser electric fields is in accordance with classical Newtonian equation (using atomic units $\hbar = e = m_{\mathrm{e}} = 1$)

$$\frac{\mathrm{d}^2 \boldsymbol{r}_i}{\mathrm{d}t^2} = -\boldsymbol{E}(t) - \nabla\left[V_{\mathrm{ne}}(\boldsymbol{r}_i) + V_{\mathrm{ee}}(\boldsymbol{r}_1, \boldsymbol{r}_2)\right], \tag{1}$$

where subscript $i = 1, 2$ denotes the index of the two electrons, and $\boldsymbol{r}_i$ is the spatial position. The term $V_{\mathrm{ne}}(\boldsymbol{r}_i) = -2/\sqrt{\boldsymbol{r}_i^2 + a^2}$ is the nucleus–electron potential energy, and $V_{\mathrm{ee}}(\boldsymbol{r}_1, \boldsymbol{r}_2) = 1/\sqrt{(\boldsymbol{r}_1 - \boldsymbol{r}_2)^2 + b^2}$ is the electron–electron interaction potential energy. In our calculations, we solve the differential equation of Newtonian motion with the fourth-fifth order Rung–Kutta algorithm and set $a = 0.1$ and $b = 0.01$ to avoid unphysical numerical singularity of computation. The external electric field is a trapezoidal shaped laser pulse with a duration of three optical cycles, which includes two cycles of platforms and one cycle of linear ramps. The expression of the pulse is

$$\boldsymbol{E}(t) = E_0 f(t)\left[\boldsymbol{e}_x \cos(\omega_x t) + \boldsymbol{e}_y \varepsilon \cos(\omega_y t + \phi)\right]. \tag{2}$$

Here, $\omega_x = 0.057$ a.u. and $\omega_y = 0.114$ a.u. are the angular frequencies of the two polarized pulses along the x and y axes, corresponding to a wavelength of 800 nm and 400 nm, respectively. $E_0 = 0.092$ a.u. is the amplitude of the external electric field, corresponding to a light intensity of 0.3 PW/cm^2. The terms ε and ϕ are the relative amplitude and initial phase of the two polarized pulses. In our calculations, the phase $\phi = 0.5\pi$ has the role of the delay between the two polarized pulses and yields high probability of double ionization. Besides, three-dimensional (3D) calculations are adopted and more than 10^7 weighted classical two-electron trajectories are traced throughout our work, resulting in over 10^4 DI events collected for statistics.

3. Numerical results and discussion

We calculated the correlated electron momentum distributions (EMDs) for the double ionization of neon atoms under an OTC electric field with an initial relative phase of 0.5π and varying relative amplitudes. The statistics on the EMD for all DI events at four different relative amplitudes, $\varepsilon = 0, 0.5, 0.75, 1$, are presented in the first column of Fig. 1. Obviously, the OTC electric field deteriorates into a polarized pulse along x axes when the relative amplitude $\varepsilon = 0$. And many typical and key DI characteristics observed in the experiments are reproduced in our simulations, as shown in Fig. 1(a1). The EMD displays a clear positive correlation, primarily distributed in the first and third quadrants. Because the generated two electrons in NSDI process tend to emit in the same direction under high laser intensity.[39] Moreover, there are a small number of anticorrelation DI events that located in the second and fourth quadrants. It is well known that, in NSDI, due to the large distribution range of recollision energy, two typical collision

pathways will coexist in the NSDI process, i.e, RII and RESI. As shown in the second and third columns of Fig. 1, we split the EMDs of all DI events into two parts according to these two different emission mechanisms. From Figs. 1(a1)–1(a3), the most conspicuous feature is that a clear V-shaped structure emerges along the diagonal in the correlated momentum spectrum when subjected to a linearly polarized laser field oriented along x axes. While this V-shaped structure can solely be observed in the RII. The reasons for this situation will be explained below. Another interesting observation in the first column of Fig. 1 is that the V-shaped structure in the correlated momentum spectrum along x axes disappears as the relative amplitude of the OTC electric field increases. Beyond that, there is a gradual rise in the probability of positive correlation events and electrons being in the low-energy region. Naturally, in RII the correlated momentum spectrum shows the same behavior as all DI events, indicating that the RII mechanism dominates for NSDI at higher laser intensity. According to previous studies, the V-shaped structure in the correlated momentum spectrum was first found by two independent experiment groups in 2007.[40] And later theoretical calculations revealed that the formation of this structure was due to the asymmetric sharing of energy between the two electrons during the collision, resulting in the correlated electron momentum spectrum displaying an off-diagonal distribution.[41]

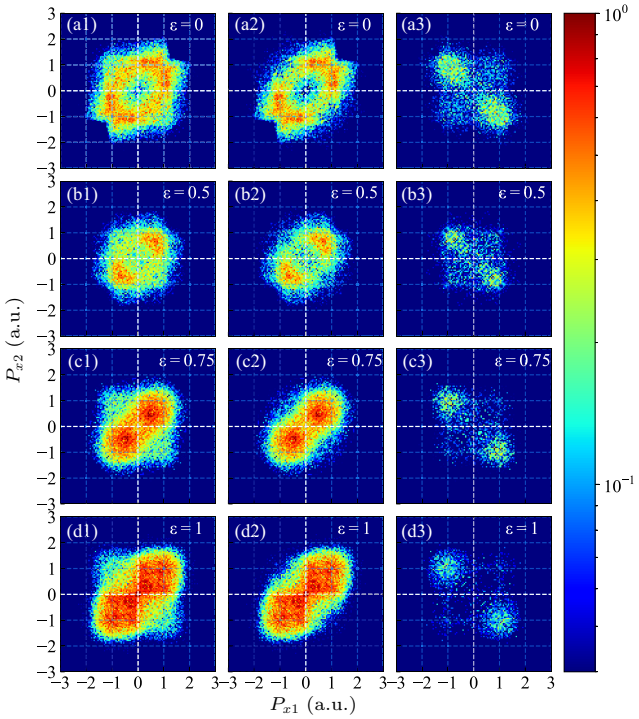


Fig. 1. The correlated electron momentum distributions (EMDs) for double ionization of neon atom in OTC field with four relative amplitudes. The values of the relative amplitudes from above to below are 0, 0.5, 0.75 and 1 respectively. [(a1), (b1), (c1), (d1)] The correlated EMDs of all DI events. [(a2), (b2), (c2), (d2)] The correlated EMDs of RII events. [(a3), (b3), (c3), (d3)] The correlated EMDs of RESI events.

To account for the responsible dynamics that V-shaped structure of the correlated electron momentum only exists in RII under a linearly polarized laser field, we tracked trajectories of DI events in RII and RESI respectively and counted the recollision time of the trajectories versus the vector potential of laser field in Fig. 2. Here, the recollision time is defined to be the instant of one tunnelling electron being first closest to the parent ion core after being driven by the laser field. Figures 2(a) and 2(b) correspond to the trajectories from Figs. 1(a2) and 1(a3), respectively. It has been observed in Fig. 2(a) that the recollision events gather near the peak of the laser field vector potential. In contrast, in Fig. 2(b) the recollision events tend to occur near the zero value of the laser field vector potential. According to the simple-man model,[15] the energy carried by one recollision electron is positively correlated with the vector potential of the laser field, which implies that the high returning-energy recollision occurs in RII, while there are lower returning-recollision in RESI.

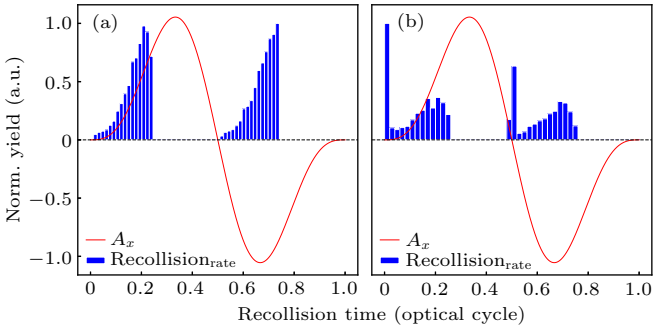


Fig. 2. The DI yield at recollision versus the vector potential of laser field in (a) RII and (b) RSEI, respectively. The blue histograms represent the DI yield at recollision and the red curves represent the vector potential of laser field.

The high returning-energy recollision often favors the asymmetric energy sharing between two electrons, creating a V-shaped structure. This is due to the recollision electron carrying high energy can quickly pass through the parent ion core and largely reduce the influence of the Coulomb focusing, resulting in the energy exchange efficiency between a recollision electron and a bound electron is lower.

Our results in Fig. 1 demonstrate that the correlated electron momentum is dependent on the relative amplitude of the OTC electric field. In order to further understand the details of dependence, in Fig. 3, we plot amplitudes (a) and Lissajous [(b), (c), (d), (e)] curves of OTC electric field with relative amplitudes are 0, 0.5, 0.75 and 1, respectively. It is clear to see that in Fig. 3(a), the amplitudes of the OTC electric field reach its lowest value ($V_{\rm min}$) 0.09 a.u. and highest value ($V_{\rm max}$) 0.12 a.u. at relative amplitudes of 0 and 1, respectively. According the ADK tunneling theory, it is known that a high intensity pulse field can induce more tunneling electrons, resulting in an increase in the probability of electron double ionization. Based on the above discussion, we can understand reason for the increase in double ionization events with relative amplitude in Fig. 1 is that the strength of the OTC electric field's amplitude increases with the relative amplitude.

Another obvious phenomenon is that the probability of electrons being in the low energy region gradually increases in the first column of Fig. 1, which should be attributed to the spreading effect of the electron wave packet. In Figs. 3(b)–3(e), we can observe that the spatial range of the electric field vector in E_x–E_y plane expands with the relative amplitude. At larger relative amplitudes, the flight time of the first tunneling electron during the recollision process becomes longer, the spread propagation of the electron wave packet becomes wider, and the energy exchange between electrons weakens, resulting in a considerable amount of low energy double ionization events.

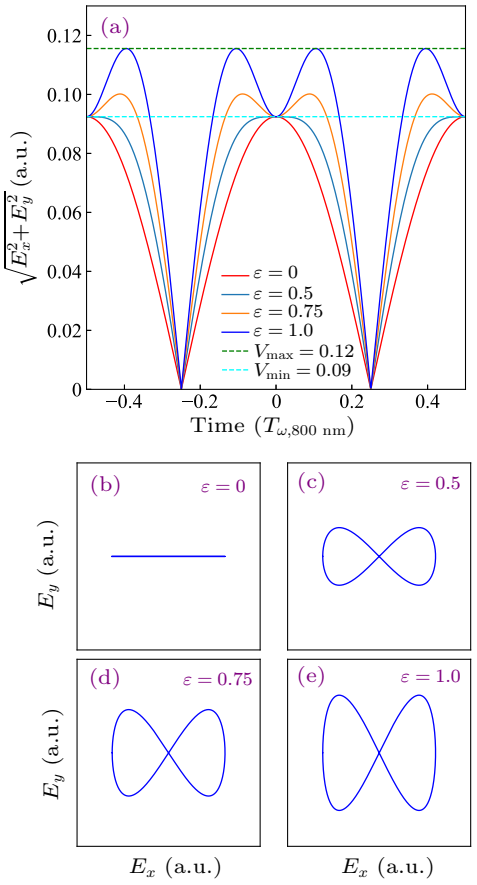


Fig. 3. The amplitudes (a) and Lissajous curves [(b)–(e)] of the OTC field with relative amplitudes are 0, 0.5, 0.75 and 1, respectively. The green dashed lines $V_{\max}$ and blue dashed lines $V_{\min}$ in the figure respectively refer to the maximum and minimum values of the peak value of the total electric field strength in a period under different relative amplitudes.

Finally, we further explore the reason for the disappearance of the V-shaped structure in the correlated momentum spectrum with increasing relative amplitude. Based on the previous discussion, we conclude that the asymmetric energy sharing during the recollision process is the decisive reason for the formation of a V-shaped structure in the longitudinal electron correlated momentum spectrum under linearly polarized laser field. To further study whether the asymmetric energy sharing is also responsible for the disappearance of the V-shaped structure in the OTC electric field, we plot the energy distribution of two electrons at 0.02 optical cycles after the collision in Fig. 4. This energy refers to the total energy of the electron, including kinetic and potential energy. Only electrons with a total energy greater than can be ionized. One issue should be noted, Fig. 4 corresponds to the DI events from Fig. 1. It is found that in the first row of Fig. 4, the energy after electrons collision is distributed very extremely off the main diagonal, implying that there is the asymmetric energy sharing between the two electrons in the collision. Furthermore, in Figs. 4(a2) and 4(a3) it can be clearly seen that the two completely different collision dynamics, that is both electrons have a high probability of direct ionization after the collision for RII, and therefore their energy is mainly distributed in the first quadrant. In contrast, for RESI, only one of the two electrons is ionized after the collision, so their energy is mainly distributed in the second, third and fourth quadrants.

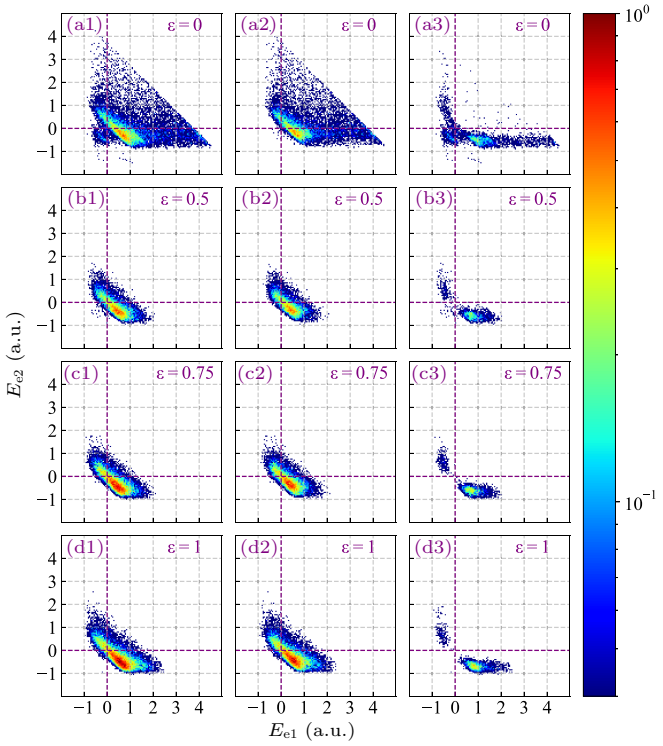


Fig. 4. The energy distributions for two electrons at 0.02 optical cycles after the collision in OTC electric field with four relative amplitudes. The values of the relative amplitudes from above to below are 0, 0.5, 0.75 and 1, respectively. [(a1), (b1), (c1), (d1)] The energy distribution of all DI events. [(a2), (b2), (c2), (d2)] The energy distribution of RII events. [(a3), (b3), (c3), (d3)] The energy distribution of RESI events.

The energy distribution becomes quite different as the relative amplitude of the OTC electric field increases. In Figs. 4(b1), 4(c1) and 4(d1), the energy distribution is clustered along the main diagonal, suggesting that the energy sharing between the two electrons after the collision is symmetric. It is well known that the Coulomb focusing effect plays a key role in electron recollision, determining the efficiency of electron–electron collision. At the relatively high laser intensity, the Coulomb focusing in transverse direction can be ne-

glected, resulting in relatively low collision efficiency. However, for the OTC electric field, electrons acquire a transverse momentum from the electric field, which plays a similar role to the Coulomb focusing effect. Consequently, the energy sharing between the electrons after collision is always symmetric even at the relatively high laser intensity, which is exactly the reason for the disappearance of the V-shaped structure.

4. Conclusions

In conclusion, we have theoretically studied the recollision dynamics in NSDI of neon atoms driven by the OTC laser field. We explore the correlation characteristics of recolliding electrons in NSDI by OTC laser field, including the correlated momentum distribution, return events and collision energy sharing, etc. Based on these results, we can conclude that for a linearly polarized laser field with relatively high laser intensity, the high returning-energy recollision mainly occurs in the RII, which is determined by the return moment of the first tunneling electron. In addition, for OTC laser fields with large relative amplitudes, the energy sharing after electrons collision is always symmetric and the yield of low-energy electrons shows a dependence on the relative amplitude. Finally, our studies indicate that changing the relative amplitude of the OTC laser field can improve the efficiency of electron–electron collisions and maintain efficient energy exchange. This means that our studies provide a way to manipulate the recollision dynamics in NSDI. We hope that our studies will serve as inspiration for further experimental studies on this topic.

Acknowledgements

Project supported by the National Natural Science Foundation of China (Grant Nos. 12204132 and 12304376), Excellent Youth Science Foundation of Shandong Province (Overseas) (Grant No. 2022HWYQ-073), the Fundamental Research Funds for the Central Universities (Grant No. HIT.OCEF.2022042), and Natural Science Foundation of Shandong Province (Grant No. ZR2023QA075).

References

[1] Pengel D, Kerbstadt S, Englert L, Bayer T and Wollenhaupt M 2017 *Phys. Rev. A* **96** 043426
[2] Pengel D, Kerbstadt S, Johannmeyer D, Englert L, Bayer T and Wollenhaupt M 2017 *Phys. Rev. Lett.* **118** 053003
[3] López S D and Arbó D G 2019 *Phys. Rev. A* **100** 023419
[4] Arbó D G, Ishikawa K L, Schiessl K, Persson E and Burgdoerfer J J P R A 2009 *Phys. Rev. A* **81** 021403
[5] Ferray M, Huillier A L, Li X F, Lompre L A, Mainfray G and Manus C 1988 *J. Phys. B: Atom. Mol. Opt. Phys.* **21** L31
[6] Krause J L, Schafer K J and Kulander K C 1992 *Phys. Rev. Lett.* **68** 3535
[7] Baker S, Robinson J S, Haworth C A, Teng H, Smith R A, Chirilă C C, Lein M, Tisch J W G and Marangos J P 2006 *Science* **312** 424
[8] Blaga C I, Xu J, DiChiara A D, Sistrunk E, Zhang K, Agostini P, Miller T A, DiMauro L F and Lin C D 2012 *Nature* **483** 194
[9] Laycock T, Olmos B, Montgomery T W A, Li W, Fromhold T M and Lesanovsky I 2013 *J. Phys. B: Atom. Mol. Opt. Phys.* **46** 245502
[10] Sun F, Lu C, Ma Y, Pan S, Wang J, Zhang W, Qiang J, Chen F, Ni H, Li H and Wu J 2021 *Opt. Express* **29** 31240
[11] Fittinghoff D N, Bolton P R, Chang B and Kulander K C 1992 *Phys. Rev. Lett.* **69** 2642
[12] Walker B, Sheehy B, DiMauro L F, Agostini P, Schafer K J and Kulander K C 1994 *Phys. Rev. Lett.* **73** 1227
[13] Song Q, Li H, Wang J, Lu P, Gong X, Ji Q, Lin K, Zhang W, Ma J, Li H, Zeng H, He F and Wu J 2018 *J. Phys. B: Atom. Mol. Opt. Phys.* **51** 074002
[14] Fittinghoff D N, Bolton P R, Chang B and Kulander K C 1992 *Phys. Rev. Lett.* **69** 2642
[15] Corkum P B 1993 *Phys. Rev. Lett.* **71** 1994
[16] Staudte A, Ruiz C, Schöffler M, Schössler S, Zeidler D, Weber T, Meckel M, Villeneuve D M, Corkum P B, Becker A and Dörner R 2007 *Phys. Rev. Lett.* **99** 263002
[17] Henrichs K, Eckart S, Hartung A, Trabert D, Fehre K, Rist J, Sann H, Pitzer M, Richter M, Kang H, Schöffler M S, Kunitski M, Jahnke T and Dörner R 2018 *Phys. Rev. A* **98** 043405
[18] Haan S L, Smith Z S, Shomsky K N and Plantinga P W 2008 *J. Phys. B: Atom. Mol. Opt. Phys.* **41** 211002
[19] Kang H, Chen S, Wang Y, Chu W, Yao J, Chen J, Liu X, Cheng Y and Xu Z 2019 *Phys. Rev. A* **100** 033403
[20] Liao Q, Lu P, Zhang Q, Yang Z and Wang X J O E 2008 *Opt. Express* **21** 17070
[21] Corkum P B 1993 *Phys. Rev. Lett.* **71** 1994
[22] Zhai C, Zhu X, Long J, Shao R, Zhang Y, He L, Tang Q, Li Y, Lan P, Yu B and Lu P 2021 *Phys. Rev. A* **103** 033114
[23] Zhang B and Lein M 2019 *Phys. Rev. A* **100** 043401
[24] Kitzler M, Xie X, Scrinzi A and Baltuska A 2007 *Phys. Rev. A* **76** 011801
[25] Kitzler M, Xie X, Roither S, Scrinzi A and Baltuska A 2008 *New J. Phys.* **10** 025029
[26] Zhang L, Xie X, Roither S, Zhou Y, Lu P, Kartashov D, Schöffler M, Shafir D, Corkum P B, Baltuška A, Staudte A and Kitzler M 2014 *Phys. Rev. Lett.* **112** 193002
[27] Zhou Y M, Huang C, Liao Q, Hong W Y and Lu P X 2011 *Opt. Lett.* **15** 2758
[28] Li Y, Qin L, Liu A, Zhang K, Tang Q, Zhai C, Xu J, Chen S, Yu B and Chen J 2022 *Chin. Phys. Lett.* **39** 093201
[29] Parker J S, Doherty B J S, Taylor K T, Schultz K D, Blaga C I and DiMauro L F 2006 *Phys. Rev. Lett.* **96** 133001
[30] Hu S X 2013 *Phys. Rev. Lett.* **111** 123003
[31] Zhu J and Scrinzi A 2020 *Phys. Rev. A* **101** 063407
[32] Jia X Y, Li W D, Fan J, Liu J and Chen J 2008 *Phys. Rev. A* **77** 063407
[33] Zhou Y, Liao Q and Lu P 2010 *Phys. Rev. A* **82** 053402
[34] Ye D F and Liu J 2010 *Phys. Rev. A* **81** 043402
[35] Sun F, Chen X, Zhang W, Qiang J, Li H, Lu P, Gong X, Ji Q, Lin K, Li H, Tong J, Chen F, Ruiz C, Wu J and He F 2020 *Phys. Rev. A* **101** 021402
[36] Pont M, Proulx D and Shakeshaft R 1991 *Phys. Rev. A* **44** 4486
[37] Ammosov M V, Delone N B and Krainov V P 1986 *J. Exp. Theor. Phys.* **64** 1191
[38] Abrines R and Percival I C 1966 *Proceedings of the Physical Society* **88** 861
[39] Haan S L, Smith Z S, Shomsky K N and Plantinga P W 2008 *J. Phys. B: Atom. Mol. Opt. Phys.* **41** 211002
[40] Staudte A, Ruiz C, Schöffler M, Schössler S, Zeidler D, Weber T, Meckel M, Villeneuve D M, Corkum P B, Becker A and Dörner R 2007 *Phys. Rev. Lett.* **99** 263002
[41] Zhou Y, Liao Q and Lu P 2010 *Phys. Rev. A* **82** 053402